



Decentralized event-based control: Stability analysis and experimental evaluation



Christian Stöcker*, Daniel Vey, Jan Lunze

Institute of Automation and Computer Control, Ruhr-Universität Bochum, Universitätsstr. 150, 44780 Bochum, Germany

ARTICLE INFO

Keywords:

Event-based control
Decentralized control
Stability analysis

ABSTRACT

Event-based control aims at reducing the amount of information which is communicated between sensors, actuators and controllers in a networked control system. The feedback link is only closed at times at which an event indicates the need for an information update to retain a desired performance. Between consecutive event times the control loop acts as a continuous system, whereas at the event times it performs a state jump. Thus, the event-based control loop belongs to the class of hybrid dynamical systems. In this paper a new method for decentralized event-based control is proposed. Two methods are presented for the stability analysis of the decentralized event-based state feedback control of physically interconnected systems. The comparison principle leads to a stability criterion that provides an upper bound for the coupling strength for which the stability of the uncoupled event-based control loops implies ultimate boundedness of the interconnected event-based system. It is shown that ultimate boundedness of the event-based state-feedback loop is implied by the asymptotic stability of the continuous state-feedback system. Furthermore, it is explained how the number of events can be reduced by estimating the interconnection signals between the subsystems and two different estimation methods are proposed. The derived methods are demonstrated for a thermofluid process by simulation and experiments.

© 2013 Elsevier Ltd. All rights reserved.

1. Introduction

1.1. Event-based control

The aim of event-based control is to reduce the communication effort between sensors, actuators and controllers by closing the control loop only at time instants t_k ($k \in \mathbb{N}_0$) when an event indicates the need for information exchange to achieve a desired closed-loop performance. The event-based control loop is a hybrid dynamical system which is characterized by a continuous state flow between the events and state resets at the event times, as explained in [1].

The system considered in this paper consists of N decentralized, and physically interconnected event-based state-feedback loops (Fig. 1). The solid lines represent continuous information transmission, whereas the dashed lines stand for the discontinuous communication at the event times t_k . Every control loop consists of a subsystem of the plant with its physical interconnection, an *event generator* (EG) that determines the event times t_k and a *control input generator* (CIG), which produces a continuous control signal between two consecutive events, based on the information received after the last event.

* Corresponding author. Tel.: +49 2343225203.

E-mail addresses: stoecker@atp.rub.de (C. Stöcker), vey@atp.rub.de (D. Vey), lunze@atp.rub.de (J. Lunze).

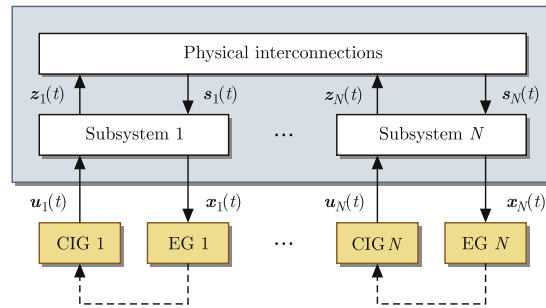


Fig. 1. Interconnected event-based control system.

The i -th subsystem is described by the linear state-space model

$$\dot{\mathbf{x}}_i(t) = \mathbf{A}_i \mathbf{x}_i(t) + \mathbf{B}_i \mathbf{u}_i(t) + \mathbf{E}_i \mathbf{s}_i(t), \quad \mathbf{x}_i(0) = \mathbf{x}_{i0} \quad (1a)$$

$$\mathbf{z}_i(t) = \mathbf{C}_{z_i} \mathbf{x}_i(t), \quad (1b)$$

in which $\mathbf{x}_i \in \mathbb{R}^{n_i}$ denotes the plant state, $\mathbf{u}_i \in \mathbb{R}^{m_i}$ the control input, $\mathbf{s}_i \in \mathbb{R}^{p_i}$ the coupling input and $\mathbf{z}_i \in \mathbb{R}^{q_i}$ the coupling output. The subsystems are interconnected according to the relation

$$\mathbf{s}(t) = \mathbf{L} \mathbf{z}(t) \quad (2)$$

with

$$\begin{aligned} \mathbf{s}(t) &= (\mathbf{s}_1^\top(t) \quad \dots \quad \mathbf{s}_N^\top(t))^\top \\ \mathbf{z}(t) &= (\mathbf{z}_1^\top(t) \quad \dots \quad \mathbf{z}_N^\top(t))^\top. \end{aligned} \quad (3)$$

The event-based state-feedback controllers are designed under the assumption of vanishing interconnections ($\mathbf{s}_i = \mathbf{0}$), hence, the N isolated event-based control loops are ultimately bounded. This paper investigates, by using the comparison principle, under what conditions on the interconnection \mathbf{L} , the stability of the subsystems implies stability of the event-based overall system. Moreover, it is presented how the number of events triggered in the overall system can be reduced by equipping the control input generators with an estimator of the interconnection signals and two estimation methods are provided. This extension of the control input generators is shown to improve the overall system performance, while on the other hand it does not affect stability.

1.2. Literature review

In recent years numerous publications have been devoted to event-based and self-triggered control approaches, see e.g. [2–5], motivated by the idea of reducing computational as well as communication effort in networked control systems. While most approaches focus on single-loop event-based control systems, the analysis of interconnected event-based control loops has been addressed only in a few publications. The behavior of event-based multi-agent systems has been investigated in [6,7], where several subsystems are not interconnected due to physical couplings but by a common control aim. Refs. [1,8] studied asynchronous measurements or controller updates in an event-based control system without explicitly considering physical interconnections between subsystems. [1] analyzed an event-based control approach for linear systems where the output of the plant and the controller can be grouped into several nodes. Using the framework of impulsive systems, stability conditions in form of linear matrix inequalities were developed. [8] studied event-based control of nonlinear systems where distributed sensor nodes transmit their measurements to a centralized control unit. The system was shown to be input-to-state stabilizable under the requirement of synchronized measurements in all components. This work has been extended in [9] in order to allow for asynchronous updates. Distributed event-based control of physically interconnected systems has been investigated in [10,11], which are discussed below in more detail. In these references triggering conditions for the subsystems were defined such that a desired decay of a Lyapunov function for the overall system is guaranteed. The stabilization of large-scale systems using distributed event-based output feedback control has been examined in [12] for passive systems.

All these approaches have in common that a zero-order hold is used to keep the control input constant between two consecutive events. In contrast to that, this paper proposes a design approach that follows the idea of [13] and yields control inputs with exponential flow, which requires a different stability analysis method than the ones which have been presented in the mentioned references, particularly regarding [10,11]. These references have proposed design methods for the triggering conditions to render the overall control system \mathcal{L}_p -stable or asymptotically stable, respectively. Besides the fact that [10,11] investigate distributed event-based control of a general class of nonlinear system, whereas this paper proposes a method for the stability analysis of decentralized event-based control of linear systems, these approaches basically differ from the present work in three points: (i) While the triggering conditions in [10,11] depend upon the system

dynamics, the threshold of the triggering condition that is used here can be freely chosen. (ii) The control aim in [10,11] is to drive the system state to the origin, whereas this approach renders the overall system ultimately bounded (i.e. once the state enters a specified target region \mathcal{X} , it remains there for all time). (iii) The main difference between [10,11] and the present work lies in the analysis approach. While [10,11] derive the stability guaranteeing triggering conditions based on requirements to a system of Lyapunov functions, this work uses the comparison principle to determine a condition that can be used to prove ultimate boundedness in dependence upon the interconnections. This condition will be shown to hold true for sufficiently weak couplings between the subsystems, which is a similarity to the approaches in [10,11], which work for weakly coupled systems, as well.

1.3. Outline of the paper

Section 2 presents an approach to decentralized event-based state-feedback control. A general condition for the stability of the event-based control system is derived in Section 3 which says that the event-based overall system is ultimately bounded if the continuous state-feedback system is proven to be asymptotically stable. In Section 4 the comparison principle is used to derive a criterion that can be used to test the stability of the composite event-based control system. Moreover, this criterion is used to determine the ultimate bound for the event-based control system. Section 5 provides a technique for improving the performance of the event-based composite system by estimating the impact of the coupling to a subsystem. The results are demonstrated in Section 6 for a thermofluid process.

1.4. Notation

\mathbb{R} and \mathbb{N} denote the set of all real or natural numbers, respectively. $\mathbb{R}_{\geq 0}$ is the set of all non-negative real numbers and $\mathbb{N}_0 = \mathbb{N} \cup \{0\}$. For a scalar s , $|s|$ denotes the absolute value. For vectors and matrices the $|\cdot|$ -operator applies to every element. For two vectors $\mathbf{v}_1, \mathbf{v}_2$ or two matrices $\mathbf{M}_1, \mathbf{M}_2$ the relations $\mathbf{v}_1 \geq \mathbf{v}_2$ or $\mathbf{M}_1 \geq \mathbf{M}_2$, respectively, holds element-wise. $\|\mathbf{x}\|_\infty$ represents the uniform norm of \mathbf{x} . The identity matrix of dimension α is represented by \mathbf{I}_α . $\lambda_p(\mathbf{A})$ denotes the Perron root of the matrix \mathbf{A} . The asterisk $*$ symbolizes the convolution operator:

$$\mathbf{G} * \mathbf{u} = \int_0^t \mathbf{G}(t - \tau) \mathbf{u}(\tau) d\tau.$$

$\mathbf{A} = \text{diag}(\mathbf{A}_1, \dots, \mathbf{A}_N)$ denotes a block diagonal matrix with the matrices \mathbf{A}_i , ($i = 1, \dots, N$) on the main diagonal. If the range of the indices i is clear from the context, this notation is abbreviated by $\mathbf{A} = \text{diag}(\mathbf{A}_i)$.

2. Decentralized event-based control

2.1. Structure of the event-based control system

This paper deals with the analysis of N interconnected event-based subsystems as shown in Fig. 1. The method presented in [13] is applied to design the decentralized event-based state-feedback controllers for the isolated subsystems

$$\dot{\mathbf{x}}_i(t) = \mathbf{A}_i \mathbf{x}_i(t) + \mathbf{B}_i \mathbf{u}_i(t), \quad \mathbf{x}_i(0) = \mathbf{x}_{i0}, \tag{4}$$

$i \in \mathcal{N} = \{1, \dots, N\}$. First, a continuous state-feedback controller

$$\mathbf{u}_i(t) = -\mathbf{K}_i \mathbf{x}_i(t) \tag{5}$$

is designed for each subsystem resulting in the isolated closed-loop subsystems

$$\dot{\mathbf{x}}_i(t) = \bar{\mathbf{A}}_i \mathbf{x}_i(t), \quad \mathbf{x}_i(0) = \mathbf{x}_{i0}, \tag{6}$$

where the matrix

$$\bar{\mathbf{A}}_i = (\mathbf{A}_i - \mathbf{B}_i \mathbf{K}_i)$$

is Hurwitz. The state-feedback gain \mathbf{K}_i is chosen such that the closed-loop system (6) has a desired performance. Both the control input generator and the event generator use the model

$$\dot{\mathbf{x}}_{si}(t) = \bar{\mathbf{A}}_i \mathbf{x}_{si}(t), \quad \mathbf{x}_{si}(t_k^+) = \mathbf{x}_i(t_k) \tag{7}$$

of the decoupled continuous reference system (6), where $\mathbf{x}_{si} \in \mathbb{R}^{m_i}$ denotes the model state and t_k^+ represents the right limit of the event time t_k at which the state of the model (7) is reset to the current plant state $\mathbf{x}_i(t_k)$.

Control input generator. The i -th control input generator uses the model (7) to generate the decentralized control input

$$\mathbf{u}_i(t) = -\mathbf{K}_i \mathbf{x}_{si}(t). \tag{8}$$

The application of the control input (8) to the i -th subsystem (1a) yields the model

$$\dot{\mathbf{x}}_i(t) = \bar{\mathbf{A}}_i \mathbf{x}_i(t) + \mathbf{B}_i \mathbf{K}_i (\mathbf{x}_i(t) - \mathbf{x}_{si}(t)) + \mathbf{E}_i \mathbf{s}_i(t), \quad \mathbf{x}_i(0) = \mathbf{x}_{i0}.$$

The coupling input $\mathbf{s}_i(t)$ generates a difference

$$\mathbf{x}_{\Delta i}(t) = \mathbf{x}_i(t) - \mathbf{x}_{si}(t), \tag{9}$$

between the model state $\mathbf{x}_{si}(t)$ and the plant state $\mathbf{x}_i(t)$. If this difference is getting larger the control input (8) may be inadequate relating to the system state $\mathbf{x}_i(t)$. Hence, the state of the model (7) needs to be reset.

Event generator. The event generator determines the time instants t_k at which a reset of the model state \mathbf{x}_{si} is necessary. It triggers an event whenever the relation

$$\|\mathbf{x}_{\Delta i}(t)\|_\infty = \|\mathbf{x}_i(t) - \mathbf{x}_{si}(t)\|_\infty = \bar{e}_i \tag{10}$$

is met, where $\bar{e}_i \in \mathbb{R}_+$ denotes the event threshold for subsystem i . At this time t_k , in the i -th event-based control loop the state of the model (7) used in both generators is reinitialized with the communicated current plant state $\mathbf{x}_i(t_k)$.

2.2. Inter-event time

This section shows that the minimum time that elapses between two consecutive events triggered within one event-based control loop, referred to as minimum inter-event time, is strictly greater than zero. Given that the overall event-based control system consists of a finite number N of subsystems, the accumulation of infinite events in finite time (Zeno behavior (cf. [14])) can be excluded.

The difference state $\mathbf{x}_{\Delta i}(t)$ is described by the state-space model

$$\dot{\mathbf{x}}_{\Delta i}(t) = \mathbf{A}_i \mathbf{x}_{\Delta i}(t) + \mathbf{E}_i \mathbf{s}_i(t), \quad \mathbf{x}_{\Delta i}(t_k^+) = \mathbf{0} \tag{11}$$

for the interval $t \in [t_k, t_{k+1})$, which yields

$$\mathbf{x}_{\Delta i}(t) = \int_{t_k}^t e^{\mathbf{A}_i(t-\tau)} \mathbf{E}_i \mathbf{s}_i(\tau) d\tau.$$

The next event is triggered at time $t = t_{k+1}$ when the difference state $\mathbf{x}_{\Delta i}(t)$ satisfies the equation

$$\|\mathbf{x}_{\Delta i}(t_{k+1})\| = \left\| \int_{t_k}^{t_{k+1}} e^{\mathbf{A}_i(t_{k+1}-\tau)} \mathbf{E}_i \mathbf{s}_i(\tau) d\tau \right\| = \bar{e}_i. \tag{12}$$

Assume that the coupling signal $\mathbf{s}_i(t)$ is bounded for all $t \geq 0$, then Eq. (12) implies that $t_{k+1} > t_k$ holds for all $k \in \mathbb{N}_0$.

Note that the application of a constant event threshold $\bar{e}_i > 0$ entails a positive inter-event time if the overall event-based control system is stable, since the coupling signal $\mathbf{s}_i(t)$ is assumed to be bounded. Section 4 derives a sufficient condition on the interconnection between the event-based control loops that guarantees stability of the overall control system and which, hence, fulfills the hypothesis of the following lemma.

Lemma 1. *Assume that the coupling signal $\mathbf{s}_i(t)$ is bounded for all $t \geq 0$. Then the minimum inter-event time for each event-based control loop is positive.*

2.3. Decentralized event-based control system

In summary, the decentralized event-based overall system consists of

- the plant (1), (2),
- N control input generators using model (7) for generating the control input (8) and
- N event generators containing model (7) which trigger an event whenever the condition (10) is satisfied.

An event in subsystem i only leads to a state reset of the models of the corresponding subsystem which causes asynchronous state resets in the overall system.

Due to an initial reset of the model states $\mathbf{x}_{si}(0)$ at time $t = 0$, $\mathbf{x}_{\Delta i}(0) = \mathbf{0}$ holds for all $i \in \mathcal{N}$. In addition, the triggering condition (10) together with the state reset causes $\mathbf{x}_{\Delta i}(t_k^+) = \mathbf{0}$ for all $k \in \mathbb{N}_0$, which implies the boundedness of the difference state (9) according to

$$|\mathbf{x}_{\Delta i}(t)| \leq (\bar{e}_i \ \cdots \ \bar{e}_i)^\top = \mathbf{e}_i, \quad \forall t \geq 0, \tag{13}$$

where \mathbf{e}_i is a vector of dimension n_i .

The decentralized event-based controllers are only known to stabilize the isolated subsystems. Hence, the main analysis problem to be solved in the following concerns the question on what condition the stability of the isolated event-based control loops implies the stability of the overall control system. This question will be answered in Section 3 by showing that any condition that is sufficient to prove the asymptotic stability of the continuous state-feedback system is likewise sufficient to prove the event-based state-feedback system to be ultimately bounded (see Definition 1 for a definition of *ultimate boundedness*). This result will be made more concrete in Section 4 which derives a stability test for the interconnected event-based control loops.

3. General stability condition

This section investigates the relation between conditions for the asymptotic stability of continuous state-feedback systems and conditions for the ultimate boundedness of event-based control systems that are realized according to the design method presented in Section 2.

Definition 1 (Ultimate Boundedness, [15]). The event-based control system (1), (2), (7), (8), (10) is said to be globally ultimately bounded (GUB) if there exists a bounded set \mathcal{X} and a time \bar{t} such that for all initial states \mathbf{x}_0 the following relation holds:

$$\exists \bar{t} : \mathbf{x}(t) \in \mathcal{X}, \quad \forall t \geq \bar{t}.$$

The following investigates the asymptotic stability of the continuous control system. First, consider the overall plant that is described by the state-space model

$$\dot{\mathbf{x}}(t) = \mathbf{A}\mathbf{x}(t) + \mathbf{B}\mathbf{u}(t), \quad \mathbf{x}(0) = \mathbf{x}_0$$

with $\mathbf{x}(t) = (\mathbf{x}_1^\top(t) \ \dots \ \mathbf{x}_N^\top(t))^\top$, $\mathbf{B} = \text{diag}(\mathbf{B}_i)$ and the matrix \mathbf{A} composed of the blocks

$$\mathbf{A}(i, j) = \begin{cases} \mathbf{A}_i & \text{for } i = j \\ \mathbf{E}_i \mathbf{L}_{ij} \mathbf{C}_{zj} & \text{for } i \neq j. \end{cases}$$

Assume that the decentralized control stations (5) are designed such that the overall controller

$$\mathbf{u}(t) = - \underbrace{\text{diag}(\mathbf{K}_1, \dots, \mathbf{K}_N)}_{:=\mathbf{K}} \mathbf{x}(t)$$

yields an asymptotically stable system

$$\frac{d}{dt} \hat{\mathbf{x}}(t) = \underbrace{(\mathbf{A} - \mathbf{BK})}_{:=\bar{\mathbf{A}}} \hat{\mathbf{x}}(t), \quad \hat{\mathbf{x}}(0) = \mathbf{x}_0$$

where the matrix $\bar{\mathbf{A}} = (\mathbf{A} - \mathbf{BK})$ is Hurwitz. The state is indicated with a hat in order to distinguish this signal from the corresponding one of the event-based control system that is investigated in the following.

Consider the event-based control system where the input is generated by means of the model

$$\begin{aligned} \dot{\mathbf{x}}_s(t) &= \bar{\mathbf{A}}\mathbf{x}_s(t), & \mathbf{x}_{si}(t_k^+) &= \mathbf{x}_i(t_k) \\ \mathbf{u}(t) &= -\mathbf{K}\mathbf{x}_s(t) \end{aligned}$$

which yields the closed-loop system

$$\begin{aligned} \dot{\mathbf{x}}(t) &= \mathbf{A}\mathbf{x}(t) - \mathbf{BK}\mathbf{x}_s(t) \\ &= \bar{\mathbf{A}}\mathbf{x}(t) + \mathbf{BK}(\mathbf{x}(t) - \mathbf{x}_s(t)). \end{aligned} \tag{14}$$

Note that the deviation between the plant state $\mathbf{x}_i(t)$ and the model state $\mathbf{x}_{si}(t)$ is bounded according to Eq. (10) for all $i \in \mathcal{N}$ which implies

$$\|\mathbf{x}(t) - \mathbf{x}_s(t)\|_\infty \leq \max_{i \in \mathcal{N}} \bar{e}_i.$$

Hence, the interconnected event-based control loops (14) are GUB, because the matrix $\bar{\mathbf{A}}$ is Hurwitz by the design of the continuous state-feedback system.

Theorem 1. Assume that the continuous control system (1), (2), (5) is asymptotically stable. Then the interconnected subsystems (1), (2) together with the decentralized event-based control stations (7), (8), which are reset whenever the condition (10) holds, is ultimately bounded.

Note that the design method proposed in Section 2 can be interpreted as an event-based implementation of a continuous decentralized state-feedback controller. This result now shows that this design method always yields an overall control system that is ultimately bounded, given that the continuous state-feedback controller renders the system asymptotically stable. The following section derives a condition that can be used to test the asymptotic stability of the continuous state-feedback system and which will be shown to be sufficient to prove the ultimate boundedness of the event-based control system. Based on this analysis the ultimate bound is explicitly determined.

4. Stability analysis using the comparison principle

4.1. Basic idea of the analysis method

This section derives a condition on the interconnection relation (2) under which the stability of the isolated event-based control loops implies stability of the overall system (1), (2), (7), (8). Note that the overall event-based control system is a hybrid dynamical system which exhibits a complex behavior that is characterized by a sequence of state jumps at the event

times and continuous dynamics in between events. Moreover, the state jumps occur asynchronously in the decentralized event-based control loops which further complicates an analysis.

In order to reduce this complexity the subsequently presented analysis first develops comparison systems for the event-based control loops. These comparison systems are linear systems that produce upper bounds on the signals that occur in the event-based control loops for all $t \geq 0$. Second, a condition for the stability of the interconnected comparison systems is derived which implies stability of the overall event-based control system. The obtained stability condition can, hence, also be used to test stability of the event-based control system.

4.2. Comparison systems

The presented stability analysis makes use of comparison systems which yield upper bounds on the signals of the respective subsystems.

Definition 2. Consider the isolated subsystem (4) that has the state trajectory

$$\mathbf{x}_i(t) = e^{\bar{A}_i t} \mathbf{x}_{i0} + \mathbf{G}_{xui} * \mathbf{u}_i,$$

where

$$\mathbf{G}_{xui}(t) = e^{\bar{A}_i t} \mathbf{B}_i \quad (15)$$

is the impulse response matrix. The system

$$\mathbf{r}_i(t) = \bar{\mathbf{F}}_i(t) |\mathbf{x}_{i0}| + \bar{\mathbf{G}}_{xui} * |\mathbf{u}_i| \quad (16)$$

with $\mathbf{r}_i \in \mathbb{R}^{n_i}$ is called a *comparison system* of subsystem (4) if it satisfies the inequality

$$\mathbf{r}_i(t) \geq |\mathbf{x}_i(t)|, \quad \forall t \geq 0$$

for an arbitrary bounded input $\mathbf{u}_i(t)$.

A method for finding a comparison system is given in the following lemma.

Lemma 2 ([16]). The system (16) is a comparison system of the system (4) if and only if the matrices $\bar{\mathbf{F}}_i(t)$ and $\bar{\mathbf{G}}_{xui}(t)$ satisfy the relations

$$\bar{\mathbf{F}}_i(t) \geq \left| e^{\bar{A}_i t} \right|, \quad \bar{\mathbf{G}}_{xui}(t) \geq |\mathbf{G}_{xui}(t)|, \quad \forall t \geq 0$$

where the impulse response matrix $\mathbf{G}_{xui}(t)$ is defined in Eq. (15).

4.3. Analysis of the continuous overall system

This section derives a method for the stability analysis for the continuous overall system (1), (2) with continuous state feedback

$$\mathbf{u}_i(t) = -\mathbf{K}_i \mathbf{x}_i(t), \quad \forall i \in \mathcal{N} \quad (17)$$

which is adapted from an analysis method that has been previously published in [16]. The method is extended in the next section to the case of event-based state-feedback control.

The controlled subsystems (1), (17) are described by the state-space models

$$\begin{aligned} \frac{d}{dt} \hat{\mathbf{x}}_i(t) &= \bar{\mathbf{A}}_i \hat{\mathbf{x}}_i(t) + \mathbf{E}_i \mathbf{s}_i(t), & \hat{\mathbf{x}}_i(0) &= \mathbf{x}_{i0} \\ \mathbf{z}_i(t) &= \mathbf{C}_{zi} \hat{\mathbf{x}}_i(t) \end{aligned} \quad (18)$$

for $i \in \mathcal{N}$, where $\hat{\mathbf{x}}_i \in \mathbb{R}^{n_i}$ denotes the state of the i -th continuous state-feedback loop. The behavior of subsystem i from input \mathbf{s}_i to state $\hat{\mathbf{x}}_i$ is given by

$$\hat{\mathbf{x}}_i(t) = e^{\bar{A}_i t} \mathbf{x}_{i0} + \mathbf{G}_{xsi} * \mathbf{s}_i$$

with

$$\mathbf{G}_{xsi}(t) = e^{\bar{A}_i t} \mathbf{E}_i. \quad (19)$$

Hence, the system

$$\mathbf{r}_{xi}(t) = \bar{\mathbf{F}}_i(t) |\mathbf{x}_{i0}| + \bar{\mathbf{G}}_{xsi} * |\mathbf{s}_i| \quad (20)$$

with

$$\bar{\mathbf{F}}_i(t) = \left| e^{\bar{\mathbf{A}}_i t} \right|, \quad \bar{\mathbf{G}}_{\text{XSi}}(t) = |\mathbf{G}_{\text{XSi}}(t)| \quad (21)$$

is a comparison system for the original system (18).

In order to investigate asymptotic stability of the overall system, set

$$\mathbf{r}_{\hat{\mathbf{x}}}(t) = (\mathbf{r}_{\hat{\mathbf{x}}1}^\top(t) \ \cdots \ \mathbf{r}_{\hat{\mathbf{x}}N}^\top(t))^\top, \quad \mathbf{x}_0 = (\mathbf{x}_{10}^\top \ \cdots \ \mathbf{x}_{N0}^\top)^\top$$

and

$$\bar{\mathbf{F}}(t) = \text{diag}(\bar{\mathbf{F}}_i(t)), \quad \bar{\mathbf{G}}_{\text{XS}}(t) = \text{diag}(\bar{\mathbf{G}}_{\text{XSi}}(t)).$$

Then the interconnection of the comparison systems (20) according to

$$|\mathbf{s}(t)| \leq |\mathbf{L}| |\mathbf{z}(t)| \leq |\mathbf{L}| |\mathbf{C}_z| |\hat{\mathbf{x}}(t)|$$

yields the comparison system for the interconnected control loops

$$\begin{aligned} \mathbf{r}_{\hat{\mathbf{x}}}(t) &= \bar{\mathbf{F}}(t) |\mathbf{x}_0| + \bar{\mathbf{G}}_{\text{XS}} * |\mathbf{s}| \\ &= \bar{\mathbf{F}}(t) |\mathbf{x}_0| + \bar{\mathbf{G}}_{\text{XS}} |\mathbf{L}| |\mathbf{C}_z| * |\hat{\mathbf{x}}| \geq |\hat{\mathbf{x}}(t)| \end{aligned} \quad (22)$$

where $\mathbf{C}_z = \text{diag}(\mathbf{C}_{zi})$. Inequality (22) is an implicit bound on the overall state $\hat{\mathbf{x}}(t)$. From the comparison principle [16] it is known that if the condition

$$\lambda_p \left(\int_0^\infty \bar{\mathbf{G}}_{\text{XS}}(t) |\mathbf{L}| |\mathbf{C}_z| dt \right) < 1 \quad (23)$$

is satisfied, the impulse response matrix

$$\mathbf{G}(t) = \delta(t) \mathbf{I}_n + \bar{\mathbf{G}}_{\text{XS}} |\mathbf{L}| |\mathbf{C}_z| * \mathbf{G} \quad (24)$$

exists and is non-negative and, hence, (22) can be rewritten in explicit form

$$\mathbf{r}_{\hat{\mathbf{x}}}(t) = \mathbf{G} * \bar{\mathbf{F}} |\mathbf{x}_0| \geq |\hat{\mathbf{x}}(t)|. \quad (25)$$

In (24), $\delta(t)$ represents the Dirac impulse and $n = \sum_{i=1}^N n_i$. The system (25) is a comparison system for the interconnected continuous control loops (2), (18). By virtue of the condition (23), $\mathbf{r}_{\hat{\mathbf{x}}}(t)$ is known to converge to zero which implies the asymptotic stability of the interconnected continuous control loops (2), (18). The following theorem summarizes the resulting stability test.

Theorem 2. Consider the interconnected continuous control loops (2), (18). If the inequality (23) is satisfied, the overall continuous state-feedback system (2), (17) is asymptotically stable.

Note that the result presented in Theorem 2 is similar to a result that has been previously published in [16]. This approach is extended in the following part to the case of event-based state-feedback which will then be used to determine the ultimate bound for the overall event-based control system.

4.4. Analysis of the event-based overall system

This section extends the previously developed stability analysis method to event-based state-feedback. Due to the event-based sampling the state of the overall hybrid system cannot be expected to converge asymptotically to the origin, but to a bounded set $\mathcal{X} \subset \mathbb{R}^n$. Hence, the subsequent analysis investigates the stability of the event-based control system in the sense of ultimate boundedness (cf. Definition 1).

The i -th subsystem (1a) with event-based control (7), (8) is described by the state-space model

$$\begin{aligned} \dot{\mathbf{x}}_i(t) &= \bar{\mathbf{A}}_i \mathbf{x}_i(t) + \mathbf{B}_i \mathbf{K}_i \mathbf{x}_{\Delta i}(t) + \mathbf{E}_i \mathbf{s}_i(t), & \mathbf{x}_i(0) &= \mathbf{x}_{i0} \\ \mathbf{z}_i(t) &= \mathbf{C}_{zi} \mathbf{x}_i(t) \end{aligned}$$

which yields the state trajectory

$$\mathbf{x}_i(t) = e^{\bar{\mathbf{A}}_i t} \mathbf{x}_{i0} + \mathbf{G}_{\text{XXi}} * \mathbf{x}_{\Delta i} + \mathbf{G}_{\text{XSi}} * \mathbf{s}_i$$

with

$$\mathbf{G}_{\text{XXi}}(t) = e^{\bar{\mathbf{A}}_i t} \mathbf{B}_i \mathbf{K}_i$$

and the difference state $\mathbf{x}_{\Delta i}(t)$ and the impulse response matrix $\mathbf{G}_{xsi}(t)$ defined in (9) or (19), respectively. An upper bound on the state $\mathbf{x}_i(t)$ is obtained by means of the comparison system

$$\mathbf{r}_{xi}(t) = \bar{\mathbf{F}}_i(t) |\mathbf{x}_{i0}| + \bar{\mathbf{G}}_{xxi} * |\mathbf{x}_{\Delta i}| + \bar{\mathbf{G}}_{xsi} * |\mathbf{s}_i| \tag{26}$$

with

$$\bar{\mathbf{G}}_{xxi}(t) = |\mathbf{G}_{xxi}(t)|$$

and $\bar{\mathbf{F}}_i(t)$ and $\bar{\mathbf{G}}_{xsi}(t)$ given in (21). As the difference state $\mathbf{x}_{\Delta i}(t)$ is bounded according to Eq. (13) the following relation holds:

$$\bar{\mathbf{G}}_{xxi} * |\mathbf{x}_{\Delta i}| = \int_0^t \bar{\mathbf{G}}_{xxi}(t - \tau) |\mathbf{x}_{\Delta i}(\tau)| d\tau \leq \mathbf{e}_{\max i}$$

with

$$\mathbf{e}_{\max i} = \int_0^\infty \bar{\mathbf{G}}_{xxi}(\tau) d\tau \cdot \mathbf{e}_i. \tag{27}$$

Given (27) the comparison system (26) can be reformulated as

$$\mathbf{r}_{xi}(t) = \bar{\mathbf{F}}_i(t) |\mathbf{x}_{i0}| + \mathbf{e}_{\max i} + \bar{\mathbf{G}}_{xsi} * |\mathbf{s}_i|.$$

Note that the difference between the upper bound on the behavior of the continuous system (20) and the event-based system (26) is only the additional term $\mathbf{e}_{\max i}$, whereas the influence of $\mathbf{s}_i(t)$ on the state $\mathbf{x}_i(t)$ remains unchanged.

A comparison system for the overall event-based control loop is obtained in the same way as for the continuous system:

$$\mathbf{r}_x(t) = \bar{\mathbf{F}}(t) |\mathbf{x}_0| + \mathbf{e}_{\max} + \bar{\mathbf{G}}_{xs} |\mathbf{L}| |\mathbf{C}_z| * |\mathbf{x}| \geq |\mathbf{x}(t)|, \tag{28}$$

where

$$\mathbf{e}_{\max} = (\mathbf{e}_{\max 1}^\top \ \cdots \ \mathbf{e}_{\max N}^\top)^\top.$$

The comparison principle is applied to Eq. (28) in order to obtain an explicit formulation of the upper bound on the state $\mathbf{x}(t)$:

$$\mathbf{r}_x(t) = \mathbf{G} * (\bar{\mathbf{F}} |\mathbf{x}_0| + \mathbf{e}_{\max}) \geq |\mathbf{x}(t)|. \tag{29}$$

Here, the impulse response matrix $\mathbf{G}(t)$ of the comparison system is given by Eq. (24) and is, hence, the same matrix as for the continuous control loop. Note that the term $\bar{\mathbf{F}} |\mathbf{x}_0|$ asymptotically vanishes, whereas \mathbf{e}_{\max} is constant. Therefore, the event-based overall system is ultimately bounded if the impulse response matrix $\mathbf{G}(t)$ satisfies the condition (23). These results are summarized in the following theorem.

Theorem 3. *The decentralized event-based control system (1), (2), (7), (8), (10) is ultimately bounded if the stability condition (23) is satisfied.*

The stability criterion (23) is a small-gain stability test. This can be seen by replacing the matrix \mathbf{L} in the interconnection relation (2) by $\gamma \mathbf{L}$ with the gain $\gamma \in \mathbb{R}_{\geq 0}$. Then condition (23) can be reformulated as

$$\lambda_p \left(\int_0^\infty \bar{\mathbf{G}}_{xs}(t) |\mathbf{L}| |\mathbf{C}_z| dt \right) < \frac{1}{\gamma},$$

which is satisfied only for sufficiently small γ .

In accordance with Theorem 1, Eq. (23) represents a sufficient condition for the asymptotic stability of the continuous closed-loop system and for the ultimate boundedness of the event-based control system. In other words, this analysis has highlighted that the event-based implementation of a decentralized state-feedback controller as proposed in Section 2 does not impose more restrictions on the interconnection relation (2) than are claimed for asymptotic stability of the continuous overall system.

4.5. Ultimate bound

Based on the previous analysis results, this section derives explicit bounds on the set \mathcal{X} in which the state $\mathbf{x}(t)$ of the event-based overall system remains for large time t . It is assumed that the sufficient stability condition (23) is satisfied. According to the comparison system (29), the state $\mathbf{x}(t)$ of the event-based overall system is bounded by

$$|\mathbf{x}(t)| \leq \mathbf{r}_x(t) = \mathbf{G} * \bar{\mathbf{F}} |\mathbf{x}_0| + \mathbf{G} * \mathbf{e}_{\max}.$$

The first term depends upon the initial state \mathbf{x}_0 and asymptotically converges to the origin, while the second term does not vanish. Hence, a limit for $\mathbf{r}_x(t)$ is given by

$$\mathbf{r}_x(t) \xrightarrow{t \rightarrow \infty} \int_0^\infty \mathbf{G}(t) dt \mathbf{e}_{\max} = \mathbf{b},$$

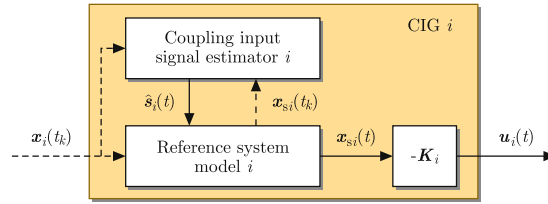


Fig. 2. Structure of the control input generator with coupling input signal estimator.

where the vector \mathbf{b} is referred to as the *ultimate bound*. Note that a value for the integral of the impulse response matrix $\mathbf{G}(t)$ follows from Eq. (24):

$$\int_0^\infty \mathbf{G}(t)dt = \left(\mathbf{I}_n - \int_0^\infty \bar{\mathbf{G}}_{xs}(t) |\mathbf{L}| |\mathbf{C}_z| dt \right)^{-1} =: \mathbf{\Gamma}.$$

Thus, the ultimate bound \mathbf{b} is

$$\mathbf{b} = \mathbf{\Gamma} \mathbf{e}_{\max} \tag{30}$$

and

$$\mathbf{x}(t) \xrightarrow{t \rightarrow \infty} \mathcal{X} := \{\mathbf{x} \mid |\mathbf{x}| \leq \mathbf{b}\} \tag{31}$$

holds.

Theorem 4. Consider the event-based overall system (1), (2), (7), (8), (10) that satisfies the stability condition (23). Then Eqs. (30), (31) define the set \mathcal{X} with ultimate bound \mathbf{b} .

5. Reduction of feedback communication effort

5.1. Extended control input generator

In the previously presented event-based control approach the control input signal for each subsystem is generated using the model (7) of a reference system that does not regard the influence of the remaining subsystems through the interconnections. The deviation between the model state $\mathbf{x}_{si}(t)$ and the plant state $\mathbf{x}_i(t)$ for subsystem i is represented by the state-space model

$$\dot{\mathbf{x}}_{\Delta i}(t) = \mathbf{A}_i \mathbf{x}_{\Delta i}(t) + \mathbf{E}_i \mathbf{s}_i(t), \quad \mathbf{x}_{\Delta i}(t_k^+) = \mathbf{0}$$

in between two consecutive events, which shows that events generated in the i -th subsystem are caused by the coupling input $\mathbf{s}_i(t)$. The difference state $\mathbf{x}_{\Delta i}(t)$ can be reduced in magnitude and, hence, events can be postponed if the model (7) takes the effect of the coupling input $\mathbf{s}_i(t)$ into account. This section proposes an extension of the control input generation by a coupling input signal estimator (Fig. 2). Instead of the model (7) the i -th control input generator now uses the model

$$\dot{\mathbf{x}}_{si}(t) = \bar{\mathbf{A}}_i \mathbf{x}_{si}(t) + \mathbf{E}_i \hat{\mathbf{s}}_i(t), \quad \mathbf{x}_{si}(t_k^+) = \mathbf{x}_i(t_k), \tag{32}$$

where $\hat{\mathbf{s}}_i \in \mathbb{R}^{p_i}$ denotes an estimation of the coupling input $\mathbf{s}_i(t)$ to the i -th subsystem. Then the deviation $\mathbf{x}_{\Delta i}(t) = \mathbf{x}_i(t) - \mathbf{x}_{si}(t)$ is described by

$$\dot{\mathbf{x}}_{\Delta i}(t) = \mathbf{A}_i \mathbf{x}_{\Delta i}(t) + \mathbf{E}_i (\mathbf{s}_i(t) - \hat{\mathbf{s}}_i(t)), \quad \mathbf{x}_{\Delta i}(t_k^+) = \mathbf{0} \tag{33}$$

for $t \in [t_k, t_{k+1})$. For an appropriate estimation $\hat{\mathbf{s}}_i(t)$, the input generation has the ability to diminish the influence of the coupling input \mathbf{s}_i on the difference state $\mathbf{x}_{\Delta i}$ and, therefore, reduces the number of events compared to the case where no coupling estimation is applied.

The i -th event generator uses the model (32) in order to check the triggering condition (10), which implies that the relation (13) still holds with the altered input generation. Since the stability analysis method presented in the previous section is independent of the particular input generator but only demands the difference state $\mathbf{x}_{\Delta i}$ to be bounded for all $i = 1, \dots, N$, the derived stability criterion is applicable to the extended event-based control system.

Subsequently, two different methods for the coupling input signal estimation are presented for which the following assumption is made.

Assumption 1. It is assumed that for the signals $\mathbf{s}_i \in \mathbb{R}^{p_i}$ and $\mathbf{x}_i \in \mathbb{R}^{n_i}$ the relation $p_i \leq n_i$ ($i = 1, \dots, N$) holds.

Note that the previous assumption is neither required for the event-based control approach without coupling input signal estimation, nor for presented stability analysis method.

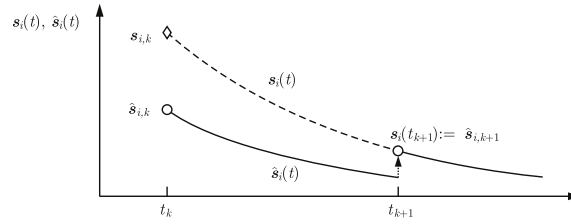


Fig. 3. Illustration of the dynamic estimation method.

5.2. Static approach to coupling signal estimation

The first estimation approach is based on the assumption that the coupling input is a piecewise constant signal

$$\mathbf{s}_i(t) = \bar{\mathbf{s}}_{i,k}, \quad \text{for } t \in [t_k, t_{k+1}). \quad (34)$$

The idea of this estimation method is as follows: At the event time t_{k+1} the coupling input estimator determines the constant signal $\bar{\mathbf{s}}_{i,k}$ which, if it has been affecting subsystem i in the time interval $t \in [t_k, t_{k+1})$, yields the difference state $\mathbf{x}_{\Delta i}(t_{k+1})$. This value $\bar{\mathbf{s}}_{i,k}$ is then used as estimation $\hat{\mathbf{s}}_i(t) = \hat{\mathbf{s}}_{i,k+1}$ for the time interval $t \geq t_{k+1}$ until the next event occurs.

Considering assumption (34), the model (33) representing the behavior of the difference state $\mathbf{x}_{\Delta i}(t)$ for $t \in [t_k, t_{k+1})$ can be rewritten as

$$\dot{\mathbf{x}}_{\Delta i}(t) = \mathbf{A}_i \mathbf{x}_{\Delta i}(t) + \mathbf{E}_i (\bar{\mathbf{s}}_{i,k} - \hat{\mathbf{s}}_{i,k}), \quad \mathbf{x}_{\Delta i}(t_k^+) = \mathbf{0},$$

which yields

$$\begin{aligned} \mathbf{x}_{\Delta i}(t) &= \int_{t_k}^t e^{\mathbf{A}_i(t-\tau)} \mathbf{E}_i (\bar{\mathbf{s}}_{i,k} - \hat{\mathbf{s}}_{i,k}) d\tau \\ &= \mathbf{A}_i^{-1} (e^{\mathbf{A}_i(t-t_k)} - \mathbf{I}_{n_i}) \mathbf{E}_i (\bar{\mathbf{s}}_{i,k} - \hat{\mathbf{s}}_{i,k}). \end{aligned}$$

At the event time t_{k+1} the difference state

$$\mathbf{x}_{\Delta i}(t_{k+1}) = \mathbf{A}_i^{-1} (e^{\mathbf{A}_i(t_{k+1}-t_k)} - \mathbf{I}_{n_i}) \mathbf{E}_i (\bar{\mathbf{s}}_{i,k} - \hat{\mathbf{s}}_{i,k})$$

is known and used to determine the new estimation according to

$$\hat{\mathbf{s}}_{i,k+1} := \bar{\mathbf{s}}_{i,k} = \hat{\mathbf{s}}_{i,k} + (\mathbf{A}_i^{-1} (e^{\mathbf{A}_i(t_{k+1}-t_k)} - \mathbf{I}_{n_i}) \mathbf{E}_i)^+ \mathbf{x}_{\Delta i}(t_{k+1}), \quad (35)$$

where $(\cdot)^+$ denotes the pseudoinverse of the indicated matrix, which exists if Assumption 1 is satisfied. Note that if the coupling input $\mathbf{s}_i(t)$ is actually constant for $t \geq t_k$, the estimation $\hat{\mathbf{s}}_{i,k+1}$ at the event time t_{k+1} obtained with (35) coincides with the actual coupling input signal $\mathbf{s}_i(t)$. This fact implies that the model state $\mathbf{x}_{\Delta i}(t)$ and the plant state $\mathbf{x}_i(t)$ behave identically for $t \geq t_{k+1}$ and no further events will be triggered.

The proposed estimation method has low computational cost as new estimations are only determined at the event times. However, this method carries the assumption that the coupling input signal $\mathbf{s}_i(t)$ is piecewise constant which might be a rough approximation, particularly if the state of the overall system is far away from the setpoint. Therefore, the next section introduces a second estimation method that takes the dynamic nature of the coupling input signal into account.

5.3. Dynamic approach to coupling signal estimation

Assume that the behavior of the coupling input $\mathbf{s}_i(t)$ is appropriately characterized in the interval $t \in [t_k, t_{k+1})$ by the linear state-space model

$$\dot{\mathbf{s}}_i(t) = \mathbf{A}_{s_i} \mathbf{s}_i(t), \quad \mathbf{s}_i(t_k) = \mathbf{s}_{i,k} \quad (36)$$

where \mathbf{A}_{s_i} is Hurwitz. The i -th coupling input signal estimator then incorporates the model

$$\frac{d}{dt} \hat{\mathbf{s}}_i(t) = \mathbf{A}_{s_i} \hat{\mathbf{s}}_i(t), \quad \hat{\mathbf{s}}_i(t_k^+) = \hat{\mathbf{s}}_{i,k} \quad (37)$$

for $t \in [t_k, t_{k+1})$ in order to determine the estimate $\hat{\mathbf{s}}_i(t)$ that is applied in the model (32) used by the control input generator.

The idea of this estimation method is illustrated in Fig. 3. Following the same arguments as for the previous estimation method, the aim is to determine at the event time t_{k+1} the initial condition $\mathbf{s}_{i,k}$ of the model (36) such that the signal $\mathbf{s}_i(t)$ for $t \in [t_k, t_{k+1})$ yields the known difference state $\mathbf{x}_{\Delta i}(t_{k+1})$. The value $\mathbf{s}_i(t_{k+1})$ is then applied as initial condition $\hat{\mathbf{s}}_{i,k+1}$ in the model (37) to get the estimate $\hat{\mathbf{s}}_i(t)$ for $t \geq t_{k+1}$.

To determine $\mathbf{s}_{i,k}$ consider the controlled subsystem for the coupling input (36)

$$\dot{\mathbf{x}}_i(t) = \mathbf{A}_i \mathbf{x}_i(t) - \mathbf{B}_i \mathbf{K}_i \mathbf{x}_i(t) + \mathbf{E}_i \mathbf{s}_i(t), \quad \mathbf{x}_i(0) = \mathbf{x}_{i0} \quad (38a)$$

$$\dot{\hat{\mathbf{s}}}_i(t) = \mathbf{A}_{s_i} \hat{\mathbf{s}}_i(t), \quad \hat{\mathbf{s}}_i(0) = \mathbf{s}_{i,0} \quad (38b)$$

and the control input generator with the coupling input (37)

$$\dot{\mathbf{x}}_{si}(t) = \bar{\mathbf{A}}_i \mathbf{x}_{si}(t) + \mathbf{E}_i \hat{\mathbf{s}}_i(t), \quad \mathbf{x}_{si}(t_k^+) = \mathbf{x}_i(t_k) \quad (39a)$$

$$\frac{d}{dt} \hat{\mathbf{s}}_i(t) = \mathbf{A}_{si} \hat{\mathbf{s}}_i(t), \quad \hat{\mathbf{s}}_i(t_k^+) = \hat{\mathbf{s}}_{i,k}. \quad (39b)$$

The difference between the behavior of the systems (38) and (39) in the interval $t \in [t_k, t_{k+1})$ is represented by the state-space model

$$\frac{d}{dt} \begin{pmatrix} \mathbf{x}_{\Delta i}(t) \\ \mathbf{s}_{\Delta i}(t) \end{pmatrix} = \begin{pmatrix} \mathbf{A}_i & \mathbf{E}_i \\ \mathbf{0} & \mathbf{A}_{si} \end{pmatrix} \begin{pmatrix} \mathbf{x}_{\Delta i}(t) \\ \mathbf{s}_{\Delta i}(t) \end{pmatrix}, \quad \begin{pmatrix} \mathbf{x}_{\Delta i}(t_k^+) \\ \mathbf{s}_{\Delta i}(t_k^+) \end{pmatrix} = \begin{pmatrix} \mathbf{0} \\ \mathbf{s}_{i,k} - \hat{\mathbf{s}}_{i,k} \end{pmatrix},$$

where $\mathbf{s}_{\Delta i} = \mathbf{s}_i - \hat{\mathbf{s}}_i$. This model yields

$$\mathbf{x}_{\Delta i}(t) = \begin{pmatrix} \mathbf{I}_{n_i} & \mathbf{0} \end{pmatrix} \begin{pmatrix} \mathbf{x}_{\Delta i}(t) \\ \mathbf{s}_{\Delta i}(t) \end{pmatrix} = \begin{pmatrix} \mathbf{I}_{n_i} & \mathbf{0} \end{pmatrix} e^{\mathbf{R}_i(t-t_k)} \begin{pmatrix} \mathbf{x}_{\Delta i}(t_k^+) \\ \mathbf{s}_{\Delta i}(t_k^+) \end{pmatrix} \quad (40)$$

with

$$\mathbf{R}_i = \begin{pmatrix} \mathbf{A}_i & \mathbf{E}_i \\ \mathbf{0} & \mathbf{A}_{si} \end{pmatrix}.$$

As

$$\begin{pmatrix} \mathbf{x}_{\Delta i}(t_k^+) \\ \mathbf{s}_{\Delta i}(t_k^+) \end{pmatrix} = \begin{pmatrix} \mathbf{0} \\ \mathbf{I}_{p_i} \end{pmatrix} (\mathbf{s}_{i,k} - \hat{\mathbf{s}}_{i,k})$$

holds, since $\mathbf{x}_{\Delta i}(t_k^+) = \mathbf{0}$ is true for all $k \in \mathbb{N}_0$, from Eq. (40)

$$\mathbf{x}_{\Delta i}(t) = \begin{pmatrix} \mathbf{I}_{n_i} & \mathbf{0} \end{pmatrix} e^{\mathbf{R}_i(t-t_k)} \begin{pmatrix} \mathbf{0} \\ \mathbf{I}_{p_i} \end{pmatrix} (\mathbf{s}_{i,k} - \hat{\mathbf{s}}_{i,k})$$

follows, which reflects the relation between the difference $\mathbf{s}_{i,k} - \hat{\mathbf{s}}_{i,k}$ and the difference state $\mathbf{x}_{\Delta i}(t)$. At the event time t_{k+1} the known difference state $\mathbf{x}_{\Delta i}(t_{k+1})$ is used to determine $\mathbf{s}_{i,k}$:

$$\mathbf{s}_{i,k} = \hat{\mathbf{s}}_{i,k} + (\mathbf{H}_i(t_{k+1} - t_k))^+ \mathbf{x}_{\Delta i}(t_{k+1}) \quad (41)$$

where

$$\mathbf{H}_i(t_{k+1} - t_k) = \begin{pmatrix} \mathbf{I}_{n_i} & \mathbf{0} \end{pmatrix} e^{\mathbf{R}_i(t_{k+1}-t_k)} \begin{pmatrix} \mathbf{0} \\ \mathbf{I}_{p_i} \end{pmatrix}.$$

The pseudoinverse of the matrix $\mathbf{H}(\cdot)$ exists if Assumption 1 is fulfilled and the matrix $\mathbf{H}^\top \mathbf{H}$ has full rank. The new initial condition for the model (37) is given by

$$\hat{\mathbf{s}}_{i,k+1} = e^{\mathbf{A}_{si}(t_{k+1}-t_k)} \mathbf{s}_{i,k}. \quad (42)$$

At time $t = 0$ the coupling input estimators are initialized with

$$\hat{\mathbf{s}}_{i,0} = \mathbf{0}, \quad \text{for all } i = 1, \dots, N.$$

In summary, the proposed coupling input estimator incorporates the model (37). At the event time t_k , the state of this model is reset according to Eqs. (41), (42) for which only the difference state $\mathbf{x}_{\Delta i}(t_k)$ needs to be known.

In general, the dynamics of the coupling input signal $\mathbf{s}_i(t)$ is only approximately represented by the model (36) which makes the matrix \mathbf{A}_{si} a design parameter. The more accurately the coupling input signal \mathbf{s}_i is estimated the less the model state \mathbf{x}_{si} deviates from the plant state \mathbf{x}_i and, thus, fewer events are triggered. A good choice of the matrix \mathbf{A}_{si} can be obtained by first identifying that subsystem (hereafter referred to as subsystem j) that has the largest impact on subsystem i and then set $\mathbf{A}_{si} = \mathbf{L}_{ij} \mathbf{C}_{zj} \mathbf{A}_j (\mathbf{L}_{ij} \mathbf{C}_{zj})^+$.

6. Example

6.1. Thermofluid process

The proposed decentralized event-based control approach is now applied to a thermofluid process depicted in Fig. 4. The process consists of two batch reactors T_1 and T_2 each of which is fed by the water supply S via the valves V_1 and V_2 . The inflow can be controlled by means of the opening angles u_{V1} and u_{V2} of the valves. The outflow from T_1 and T_2 to W_1 or W_2 , respectively, is constant. The temperature in reactor T_1 can be reduced by means of the cooling unit and can be increased in reactor T_2 by means of the heating rods using the control signals u_c or u_H , respectively. Both reactors are defined as subsystems which are coupled through flows from T_1 to T_2 and vice versa. The strength of these couplings depends on the

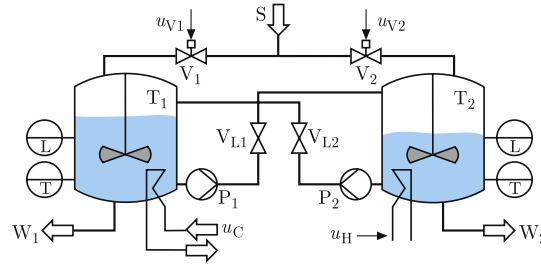


Fig. 4. Thermofluid process.

opening angles of the valves V_{L1} and V_{L2} . The control aim is to keep the temperature ϑ , measured in Kelvin and level l of the liquid, measured in centimeters, constant in both reactors, using decentralized event-based controllers.

With the states

$$\mathbf{x}_1 = (l_{T1} \quad \vartheta_{T1})^\top, \quad \mathbf{x}_2 = (l_{T2} \quad \vartheta_{T2})^\top$$

and control inputs

$$\mathbf{u}_1 = (u_{V1} \quad u_{H1})^\top, \quad \mathbf{u}_2 = (u_{V2} \quad u_{H2})^\top$$

the system is described by the linearized state-space model (1) with

$$\begin{aligned} \mathbf{A}_1 &= 10^{-3} \begin{pmatrix} -5.74 & 0 \\ -34.5 & -8.58 \end{pmatrix}, & \mathbf{A}_2 &= 10^{-3} \begin{pmatrix} -5.00 & 0 \\ 39.2 & -5.58 \end{pmatrix} \\ \mathbf{B}_1 &= 10^{-3} \begin{pmatrix} 2.30 & 0 \\ 0 & -38.9 \end{pmatrix}, & \mathbf{B}_2 &= 10^{-3} \begin{pmatrix} 2.59 & 0 \\ 0 & 35.0 \end{pmatrix} \\ \mathbf{E}_1 &= 10^{-3} \begin{pmatrix} 2.42 & 0 \\ 43.9 & 5.44 \end{pmatrix}, & \mathbf{E}_2 &= 10^{-3} \begin{pmatrix} 2.85 & 0 \\ -46.5 & 5.58 \end{pmatrix} \\ \mathbf{C}_{z1} &= \begin{pmatrix} 1 & 0 \\ 0 & 1 \end{pmatrix}, & \mathbf{C}_{z2} &= \begin{pmatrix} 1 & 0 \\ 0 & 1 \end{pmatrix} \end{aligned}$$

which is valid around the setpoint $\bar{\mathbf{x}}_1 = (0.33 \quad 295)^\top$ and $\bar{\mathbf{x}}_2 = (0.34 \quad 300)^\top$, where the level and the temperature are measured in m or K, respectively. A symmetric interconnection between both subsystems is modeled by the relation (2) with

$$\mathbf{L} = \begin{pmatrix} \mathbf{0} & \mathbf{L}_{12} \\ \mathbf{L}_{21} & \mathbf{0} \end{pmatrix} = \kappa \begin{pmatrix} \mathbf{0} & \mathbf{I}_{q_1} \\ \mathbf{I}_{q_2} & \mathbf{0} \end{pmatrix},$$

where $\kappa \in \mathbb{R}_{\geq 0}$ represents a coupling parameter that is related to the opening angles of the valves V_{L1} and V_{L2} . The decentralized state-feedback controller $\mathbf{K} = \text{diag}(\mathbf{K}_1, \mathbf{K}_2)$ with

$$\mathbf{K}_1 = \begin{pmatrix} 7.280 & 0 \\ 0.89 & -0.08 \end{pmatrix}, \quad \mathbf{K}_2 = \begin{pmatrix} 7.73 & 0 \\ 1.12 & 0.05 \end{pmatrix}$$

ensures stability of the decoupled subsystems, i.e. for $\kappa = 0$. For the event-based implementation of this controller the event thresholds

$$\bar{e}_1 = \bar{e}_2 = 0.5$$

are chosen.

6.2. Stability analysis of the thermofluid process

The following paragraph investigates the stability of the event-based overall system. The stability test (23) fails for interconnections that are larger than the critical value $\kappa_{\text{crit}} = 1.68$. The analysis of the eigenvalues of the continuous control loop reveals that the overall system in fact becomes unstable for $\kappa \geq 1.69 = \tilde{\kappa}_{\text{crit}}$ which, according to Theorem 1, implies instability of the event-based control loop. The fact that $\kappa_{\text{crit}} \approx \tilde{\kappa}_{\text{crit}}$ shows that the small-gain test (23) yields excellent results if the impulse response matrices are nearly non-negative such that the $|\cdot|$ -operator has minor effect on the analysis result.

6.3. Simulation results

The behavior of the event-based overall system is now investigated for interconnections with $\kappa = 1.5$ and initial condition

$$\mathbf{x}_1(0) = (0.05 \quad 5)^\top, \quad \mathbf{x}_2(0) = (-0.05 \quad -5)^\top.$$

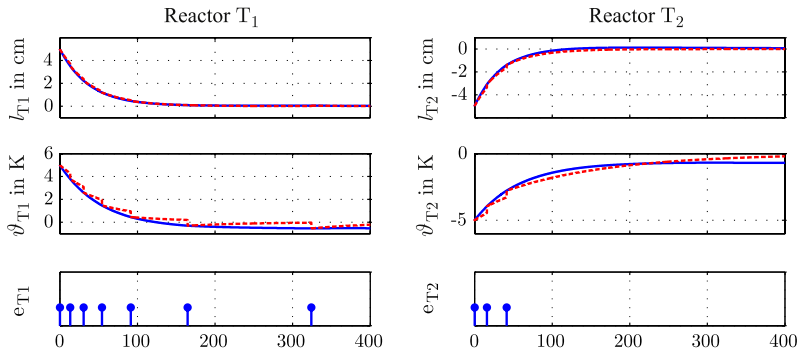


Fig. 5. Behavior of the event-based control system.

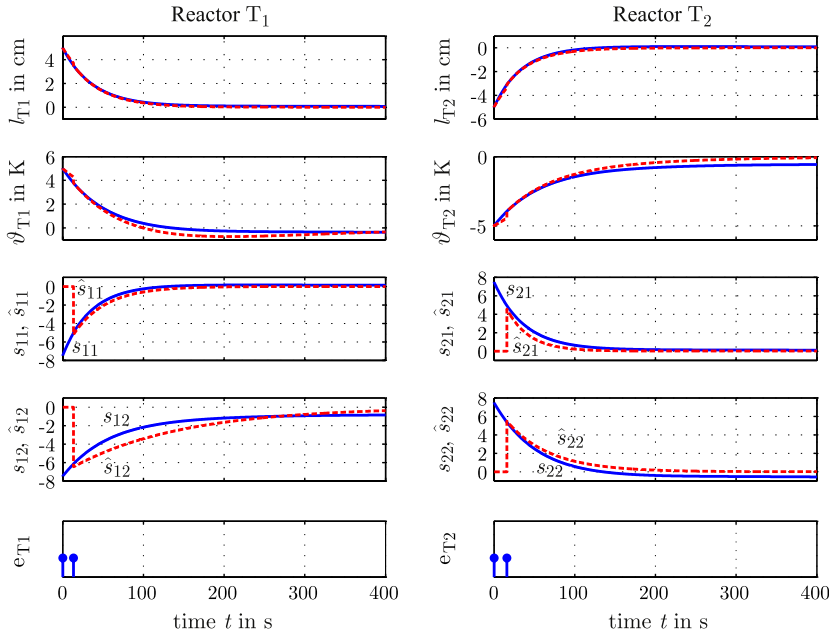


Fig. 6. Behavior of the event-based control system with coupling signal estimation.

Fig. 5 depicts the simulation results for the case where no coupling input estimator is applied in the control input generator. The left-hand side shows the trajectories of the level l_{T1} and temperature ϑ_{T1} (first and second figure from top) of the liquid in reactor T_1 and the right-hand side gives the respective trajectories of the level l_{T2} and temperature ϑ_{T2} in reactor T_2 . The solid lines represent the plant states and the dashed lines the model states. The model state in each subsystem is reset after every event. The generated events are symbolized by the stems at the bottom of the figure. In this example 10 events are triggered solely caused by a difference between the temperatures of the plant and the model. This is due to the fact that the symmetric interconnection has no influence on the behavior of the reactor levels.

The advantage of the dynamic coupling input signal estimation that was presented in Section 5.3 is illustrated in Fig. 6, which shows the behavior of the overall event-based control system for the same coupling strength and initial condition as in the previously investigated case. The left-hand side of Fig. 6 depicts the trajectories of the level l_{T1} and temperature ϑ_{T1} of the liquid in reactor T_1 as well as the coupling input signals $\mathbf{s}_1(t)$ and $\mathbf{s}_2(t)$ (solid lines) and its estimates $\hat{\mathbf{s}}_1(t)$ or $\hat{\mathbf{s}}_2(t)$ (dashed lines), respectively. The right-hand side of Fig. 6 shows the corresponding signals of the reactor T_2 .

For the coupling input estimation for both subsystems the model (37), (41), (42) is used with

$$\begin{aligned} \mathbf{A}_{s1} &= \mathbf{L}_{12}\mathbf{C}_{z2}\bar{\mathbf{A}}_2(\mathbf{L}_{12}\mathbf{C}_{z2})^+ = \bar{\mathbf{A}}_2, \\ \mathbf{A}_{s2} &= 1.6 \cdot \mathbf{L}_{21}\mathbf{C}_{z1}\bar{\mathbf{A}}_1(\mathbf{L}_{21}\mathbf{C}_{z1})^+ = 1.6 \cdot \bar{\mathbf{A}}_1. \end{aligned}$$

The simulation results show that by including this estimation into the control input generation the total number of events can be reduced significantly compared to the case without estimation. Besides the initial events, only one event is triggered in each event-based control loop. After the second event has been triggered in each of the event-based control loops, the estimations $\hat{\mathbf{s}}_1(t)$ and $\hat{\mathbf{s}}_2(t)$ approximate the actual coupling signals $\mathbf{s}_1(t)$ or $\mathbf{s}_2(t)$, respectively, with sufficient precision, such that the model states almost coincide with the plant states and, hence, no further event is generated.

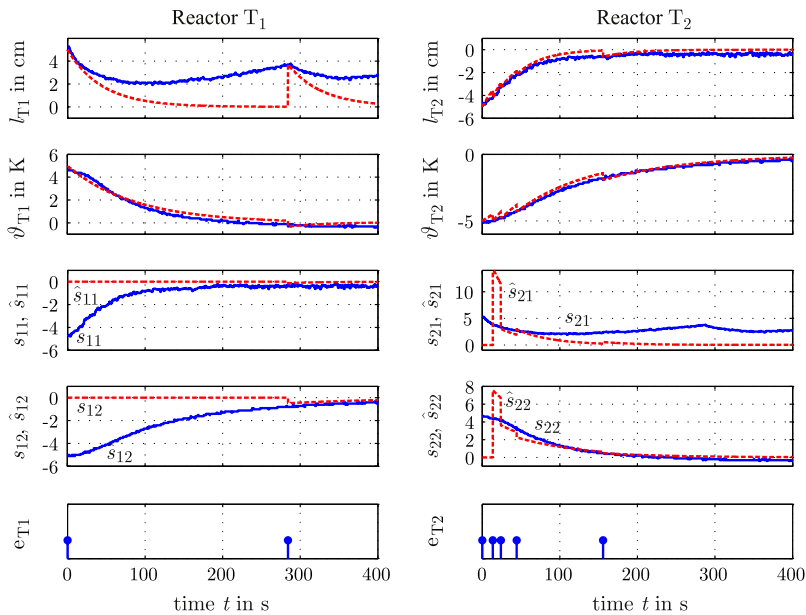


Fig. 7. Behavior of the event-based control system in the experiment.

Note that the factor 1.6 for the choice of the matrix \mathbf{A}_{s2} was used in order to further improve the dynamic coupling input signal estimation. For the choice $\mathbf{A}_{s2} = \bar{\mathbf{A}}_1$, two more events would have been triggered in the second subsystem.

6.4. Experimental evaluation

Fig. 7 illustrates the experimental results of the investigation of the event-based state-feedback system with dynamic coupling input signal estimation for interconnections with $\kappa = 1$. In comparison with Fig. 6, it can be observed that in the experiment three more events are triggered in the second subsystem. The difference between the simulation and the experiment mainly rests on model uncertainties. This is also the reason for the deviation between the plant state and the model state of the level l_{T1} in reactor T_1 . Nevertheless, the experiment shows that the event-based state-feedback approach works well together with the dynamic coupling input signal estimation and, moreover, is robust with respect to model uncertainties.

7. Conclusion

The paper has presented a new method for decentralized event-based control together with two stability tests showing that continuous decentralized controllers can be emulated by event-based controllers with arbitrary accuracy if the event generators and the control input generators are designed for the isolated subsystems by means of the method described by [13]. If the continuous system is asymptotically stable, the event-based system is ultimately bounded, where the bound depends upon the event thresholds.

References

- [1] M.C.F. Donkers, W.P.M.H. Heemels, Output-based event-triggered control with guaranteed \mathcal{L}_∞ -gain and improved and decentralised event-triggering, *IEEE Trans. Automat. Control* 57 (2012) 1362–1376.
- [2] K.-E. Årzén, A simple event-based PID controller, in: Preprints 14th IFAC World Congress, pp. 423–428.
- [3] K.J. Åström, B. Bernhardsson, Comparison of Riemann and Lebesgue sampling for first order stochastic systems, in: Proc. IEEE Conf. Decision & Control, pp. 2011–2016.
- [4] P. Tabuada, Event-triggered real-time scheduling of stabilizing control tasks, *IEEE Trans. Automat. Control* 52 (2007) 1680–1685.
- [5] W.P.M.H. Heemels, J.H. Sandee, P.P.J. van den Bosch, Analysis of event-driven controllers for linear systems, *Internat. J. Control* 81 (2008) 571–590.
- [6] D. Dimarogonas, E. Frazzoli, K. Johansson, Distributed event-triggered control for multi-agent systems, *IEEE Trans. Automat. Control* 57 (2012) 1291–1297.
- [7] G. Seyboth, D. Dimarogonas, K. Johansson, Event-based broadcasting for multi-agent average consensus, *Automatica* 49 (2013) 245–252.
- [8] M. Mazo, P. Tabuada, Decentralized event-triggered control over wireless sensor/actuator networks, *IEEE Trans. Automat. Control* 56 (2011) 2455–2461.
- [9] M. Mazo, M. Cao, Decentralized event-triggered control with one bit communications, in: Proc. 4th IFAC Conf. Analysis and Design of Hybrid Systems, pp. 52–57.
- [10] X. Wang, M.D. Lemmon, Event-triggering in distributed networked control systems, *IEEE Trans. Automat. Control* 56 (2011) 586–601.
- [11] C. De Persis, R. Sailer, F. Wirth, Parsimonious event-triggered distributed control: a zero free approach, *Automatica* (2013) <http://dx.doi.org/10.1016/j.automatica.2013.03.003>.

- [12] H. Yu, F. Zhu, P.J. Antsaklis, Stabilization of large-scale distributed control systems using I/O event-driven control and passivity, in: Proc. 50th IEEE Conf. Decision & Control, pp. 4245–4250.
- [13] J. Lunze, D. Lehmann, A state-feedback approach to event-based control, *Automatica* 46 (2010) 211–215.
- [14] J. Lunze, F. Lamnabhi-Lagarrigue (Eds.), *Handbook of Hybrid Systems Control*, Cambridge University Press, 2009.
- [15] H.K. Khalil, *Nonlinear Systems*, third ed., Prentice-Hall, 2002.
- [16] J. Lunze, *Feedback Control of Large-Scale Systems*, Prentice Hall, Upper Saddle River, NJ, 1992.